Comparison of the Auxiliary Density Perturbation Theory and the Noniterative Approximation to the Coupled Perturbed Kohn−Sham Method: Case Study of the Polarizabilities of Disubsti...

ARTICLE *in* THE JOURNAL OF PHYSICAL CHEMISTRY A · FEBRUARY 2010

Impact Factor: 2.69 · DOI: 10.1021/jp909966f · Source: PubMed

4 AUTHORS, INCLUDING:

Sapana V. Shedge
University of Geneva
10 PUBLICATIONS **34** CITATIONS
SEE PROFILE

Sourav Pal
CSIR - National Chemical Laboratory, Pune
180 PUBLICATIONS **2,823** CITATIONS
SEE PROFILE

Comparison of the Auxiliary Density Perturbation Theory and the Noniterative Approximation to the Coupled Perturbed Kohn−Sham Method: Case Study of the Polarizabilities of Disubstituted Azoarene Molecules

Sapana V. Shedge,[†] Javier Carmona-Espíndola,[‡] Sourav Pal,*[,†] and Andreas M. Köster*[,‡]

[†] *Theory Group, Physical Chemistry Division, National Chemical Laboratory, Pune 411 008, India, and* [‡] *Departamento de Química, CINVESTAV, Avenida Instituto Politécnico Nacional 2508, A.P. 14-740, México D.F. 07000, México*

Received: October 18, 2009; Revised Manuscript Received: December 26, 2009

We present a theoretical study of the polarizabilities of free and disubstituted azoarenes employing auxiliary density perturbation theory (ADPT) and the noniterative approximation to the coupled perturbed Kohn−Sham (NIA-CPKS) method. Both methods are noniterative but use different approaches to obtain the perturbed density matrix. NIA-CPKS is different from the conventional CPKS approach in that the perturbed Kohn−Sham matrix is obtained numerically, thereby yielding a single-step solution to CPKS. ADPT is an alternative approach to the analytical CPKS method in the framework of the auxiliary density functional theory. It is shown that the polarizabilities obtained using these two methods are in good agreement with each other. Comparisons are made for disubstituted azoarenes, which give support to the push−pull mechanism. Both methods reproduce the same trend for polarizabilities because of the substitution pattern of the azoarene moiety. Our results are consistent with the standard organic chemistry "activating/deactivating" sequence. We present the polarizabilities of the above molecules calculated with three different exchange-correlation functionals and two different auxiliary function sets. The computational advantages of both methods are also discussed.

1. Introduction

Density functional theory (DFT)[1–3] has been used extensively for calculation of the molecular response properties of a wide variety of atoms, molecules, and clusters. Many other approaches such as coupled-cluster (CC) and time-dependent self-consistent field procedures,[4,5] the popular coupled-perturbed Hartree−Fock approach,[6] and the time-dependent Hartree−Fock-based perturbation scheme[7] are also available for property calculations. However, among these, DFT has been widely used. While the DFT approach is exact in principle, the popularity of the approach is mainly due to the simple working equations arising from the use of the electron density as the basic variable in the entire framework of the theory. Electron correlation effects and basis sets play important roles in the determination of response properties. DFT is well suited for large molecules and large basis sets, and it takes care of electron correlation. However, it scales similarly to the Hartree−Fock theory in terms of computational demand when hybrid functionals are used. DFT calculations without such functionals can, with intelligent use of Fourier transforms or auxiliary basis sets, scale significantly better than Hartree−Fock calculations. The true practical applicability of DFT comes from the introduction of a fictitious noninteracting reference system as proposed by Kohn and Sham.[8] This circumvents the explicit construction of the unknown kinetic energy functional and guarantees the accuracy of the approach. Electric properties of molecules are studied to understand their response to an external weak perturbation. Typical examples are molecular dipole polarizabilities and hyperpolarizabilities. Several studies of molecules[9–19] and solids[20] have found that DFT is well suited for these property calculations. More recently, even temperature-dependent polarizabilities were studied by first-principle DFT Born−Oppenheimer molecular dynamics simulations.[21]

The response of a molecule to an electric field perturbation in terms of the electron density is given by the derivative of the density with respect to the electric field components. These derivatives or density responses can be obtained self-consistently for variational energy expressions. The variational equations transcribed in a basis set expansion involve the derivatives of the Kohn−Sham matrix and can be shown to be equivalent to the coupled perturbed Kohn−Sham (CPKS) equations. The response property can also be calculated using linear response time-dependent DFT (LR-TDDFT).[22–28] The precise relationship between these two approach is discussed in the literature.[29,30] There is no difference, however, between the LR-TDDFT and CPKS approach for static response properties with fixed basis sets, which is the case here. The CPKS method has proven to be very useful for response property calculations.[31,32] In the Kohn−Sham formalism, the analytical derivative approach requires the solution of the CPKS equations in order to obtain the first-order response of the molecular electron density. The CPKS equations involve evaluation of the functional derivative of the exchange-correlation potential for construction of the Kohn−Sham matrix derivative. Because the Kohn−Sham matrix derivatives depend on the perturbed density, the CPKS equations need to be solved in an iterative manner. This involves the transformation of molecular integrals from the original atomic orbital basis to the molecular orbital basis. As a result, the straightforward evaluation of second-order response equations in DFT scales formally as N^5, where N denotes the number of basis functions in the system. Thus, for large molecules, this approach is not feasible. This situation has motivated us to put forth new formalisms in which the CPKS equation can be solved in a single

* E-mail: akoster@cinvestav.mx (A.M.K.), s.pal@ncl.res.in (S.P.).

10.1021/jp909966f
Published on Web 01/20/2010

step. One of them is the so-called noniterative approximation to the CPKS (NIA-CPKS) method.[33–37] Here the derivative of the Kohn−Sham matrix is obtained by a finite-field approximation, and it is used in the CPKS equation to calculate the perturbed density matrix for polarizability calculations. It is a numerical−analytical method because only the derivative of the Kohn−Sham matrix is obtained numerically. The standard finite-field method[38] already implemented in deMon2k is different from the NIA-CPKS method in that the energy derivatives are obtained numerically. The other noniterative approach that we discuss in this paper is auxiliary density perturbation theory (ADPT),[39] where the perturbed density matrix is obtained noniteratively by solving an inhomogeneous equation system with the dimension of the number of auxiliary functions used to expand the approximated density. ADPT is derived from self-consistent perturbation (SCP) theory[40–45] in the framework of the auxiliary DFT (ADFT) method.[39,46] Both methods are implemented in deMon2k,[47] which permits a direct comparison.

The main aim of the comparison presented here is to validate the reliability of approximated density approaches for perturbation calculations, in particular the calculation of polarizabilities, for electronically more complicated systems. Because of their technological importance,[48–58] we have selected azoarenes for this study. They are classical push−pull systems with large polarizabilities and hyperpolarizabilities.[59–62] For the comparison, the local density approximation as well as the generalized gradient approximation (GGA) is employed. Thus, for the first time, ADPT GGA polarizabilities are reported. The article is organized in the following manner. In the next section, the theories of ADPT and NIA-CPKS are briefly reviewed. The computational details are described in section 3. The calculated ADPT, NIA-CPKS, and finite-field perturbation (FFP) polarizabilities are compared and discussed in the following section. Final conclusions are drawn in section 5. The implementation details for the numerical kernel calculations in ADPT are given in the appendix.

2. Theory

2.1. ADPT. The Kohn−Sham SCF energy expression is given as

$$E_{\mathrm{SCF}} = \sum_{\mu,\nu} P_{\mu\nu} H_{\mu\nu} + \frac{1}{2} \sum_{\mu,\nu} \sum_{\sigma,\tau} P_{\mu\nu} P_{\sigma\tau} \langle \mu\nu || \sigma\tau \rangle + E_{\mathrm{xc}}[\rho] \tag{1}$$

where $P_{\mu\nu}$ is an element of the density matrix and$H_{\mu\nu}$ that of the core Hamiltonian. The core Hamiltonian contains kinetic energy and nuclear attraction integrals as well as one-electron perturbation terms. The second term in (1) represents the classical Coulomb repulsion between the electrons and involves four-center electron−electron repulsion integrals. In our notation, the two-electron Coulomb operator is denoted by the || symbol. The last term represents the exchange-correlation energy. In deMon2k,[47] auxiliary functions are used to fit the charge density. The approximate density $\tilde{\rho}(r)$ is expanded into primitive Hermite Gaussians $\bar{k}(r)$ centered on atoms[63,64] as

$$\tilde{\rho}(r) = \sum_{\bar{k}} x_{\bar{k}} \bar{k}(r) \tag{2}$$

Here the primitive Hermite Gaussian auxiliary functions are denoted by a bar. The above auxiliary density is used for the variational fitting of the Coulomb potential.[65,66] As a result, the N^4 scaling of the Coulomb integrals is avoided. In ADFT, the approximated density is also used for calculation of the exchange-correlation energy.[67] The ADFT energy expression is given as

$$E_{\mathrm{SCF}} = \sum_{\mu,\nu} P_{\mu\nu} H_{\mu\nu} + \sum_{\mu,\nu} \sum_{\bar{k}} P_{\mu\nu} \langle \mu\nu || \bar{k} \rangle x_{\bar{k}} - \frac{1}{2} \sum_{\bar{k},\bar{l}} x_{\bar{k}} x_{\bar{l}} \langle \bar{k} || \bar{l} \rangle + E_{\mathrm{xc}}[\tilde{\rho}] \tag{3}$$

The fitting coefficients $x_{\bar{k}}$ are obtained by the variational minimization of the difference between the Kohn−Sham and auxiliary densities in a Coulomb metric according to Dunlap et al.[68] Different from the original work of Dunlap et al., no charge conservation constraint is employed.[27] As a result, the following inhomogeneous equation system[69] for determination of the fitting coefficients collected in the vector **x** is obtained:

$$\mathbf{G}\mathbf{x} = \mathbf{J} \tag{4}$$

Here **G** and **J** denote the Coulomb matrix and vector. They are defined as

$$G_{\bar{k}\bar{l}} = \langle \bar{k} || \bar{l} \rangle \tag{5}$$

$$J_{\bar{k}} = \sum_{\mu,\nu} P_{\mu\nu} \langle \mu\nu || \bar{k} \rangle \tag{6}$$

The formal solution to this equation is given by[69]

$$x_{\bar{k}} = \sum_{\bar{l}} G_{\bar{k}\bar{l}}^{-1} J_{\bar{l}} = \sum_{\bar{l}} \sum_{\mu,\nu} \langle \bar{k} || \bar{l} \rangle^{-1} \langle \bar{l} || \mu\nu \rangle P_{\mu\nu} \tag{7}$$

For calculation of the exchange-correlation contribution in ADFT, it is convenient to introduce a second set of fitting coefficients. These so-called exchange-correlation fitting coefficients are given by[39]

$$z_{\bar{k}} \equiv \sum_{\bar{l}} \langle \bar{k} || \bar{l} \rangle^{-1} \langle \bar{l} | v_{\mathrm{xc}}[\tilde{\rho}] \rangle \tag{8}$$

It should be noted that calculation of the exchange-correlation fitting coefficients involves a numerical integration and that these coefficients are usually spin-polarized. The ADFT Kohn−Sham matrix elements are then given as

$$K_{\mu\nu} = H_{\mu\nu} + \sum_{\bar{k}} \langle \mu\nu || \bar{k} \rangle (x_{\bar{k}} + z_{\bar{k}}) \tag{9}$$

As can be seen from the above equation, the ADFT Kohn−Sham matrix elements depend only on the Coulomb and exchange-correlation coefficients. Thus, only the approximated density is numerically calculated on a grid. Because this density is linearly scaled by construction, the necessary grid work is considerably reduced. In fact, calculation of the Kohn−Sham potential is in ADFT identical with orbital-free DFT approaches, with the auxiliary density as the basic variable. This also has significant importance for calculation of the higher energy derivatives, as we will now show.

For second energy derivatives, the perturbed density matrix must be calculated. For closed-shell systems, this matrix can be obtained from the SCP theory as follows:

$$P_{\mu\nu}^{(\lambda)} \equiv \frac{\partial P_{\mu\nu}}{\partial\lambda} = 2\sum_{i}^{\text{occ}}\sum_{a}^{\text{uno}} \frac{\mathbf{K}_{ia}^{(\lambda)} - \varepsilon_i S_{ia}^{(\lambda)}}{\varepsilon_i - \varepsilon_a}(c_{\mu i}c_{\nu a} + c_{\mu a}c_{\nu i}) - \frac{1}{2}\sum_{\sigma,\tau} P_{\mu\sigma}S_{\sigma\tau}^{(\lambda)}P_{\tau\nu} \quad (10)$$

The overlap matrix derivatives in eq 10 vanish in the case of perturbation-independent basis set and auxiliary functions discussed here, and the expression for the perturbed density matrix elements simplifies to

$$P_{\mu\nu}^{(\lambda)} = 2\sum_{i}^{\text{occ}}\sum_{a}^{\text{uno}} \frac{\mathbf{K}_{ia}^{(\lambda)}}{\varepsilon_i - \varepsilon_a}(c_{\mu i}c_{\nu a} + c_{\mu a}c_{\nu i}) \quad (11)$$

Here λ is the perturbation parameter, which in our case represents an electric field component, and ε_i and ε_a are orbital energies of the ith occupied and ath unoccupied orbitals. The superscript notation refers always to partial derivatives, i.e., does not affect molecular orbital coefficients in molecular integral transformations. The perturbed Kohn−Sham matrix $\mathbf{K}_{ia}^{(\lambda)}$ is given in the molecular orbital representation as

$$K_{ia}^{(\lambda)} = \sum_{\mu,\nu} c_{\mu i}c_{\nu i}K_{\mu\nu}^{(\lambda)} \quad (12)$$

with

$$K_{\mu\nu}^{(\lambda)} = H_{\mu\nu}^{(\lambda)} + \sum_{\bar{k}} \langle\mu\nu||\bar{k}\rangle(x_{\bar{k}}^{(\lambda)} + z_{\bar{k}}^{(\lambda)}) \quad (13)$$

The perturbed exchange-correlation coefficients are given by

$$z_{\bar{k}}^{(\lambda)} = \sum_{\bar{l}} \langle\bar{k}||\bar{l}\rangle^{-1}\langle\bar{l}|v_{\text{xc}}^{(\lambda)}[\tilde{\rho}]\rangle \quad (14)$$

Because $v_{\text{xc}}^{(\lambda)}[\tilde{\rho}]$ is a functional of the approximated density, it follows that

$$\langle\bar{l}|v_{\text{xc}}^{(\lambda)}[\tilde{\rho}]\rangle = \int\int \bar{l}(r)\frac{\delta v_{\text{xc}}[\tilde{\rho}]}{\delta\tilde{\rho}(r')}\frac{\partial\tilde{\rho}(r')}{\partial\lambda}\,\mathrm{d}r\,\mathrm{d}r'$$

$$= \sum_{\bar{m}} \langle\bar{l}|f_{\text{xc}}[\tilde{\rho}]|\bar{m}\rangle x_{\bar{m}}^{(\lambda)} \quad (15)$$

Compared to the standard kernel of linear combination of Gaussian-type orbitals, the scaling of the ADPT kernel integrals is reduced by 2 orders of magnitude. The exchange-correlation kernel $f_{\text{xc}}[\tilde{\rho}]$ is defined as the second derivative of the exchange-correlation energy:

$$f_{\text{xc}}[\tilde{\rho}(r),\tilde{\rho}(r')] \equiv \frac{\delta^2 E_{\text{xc}}[\tilde{\rho}]}{\delta\tilde{\rho}(r)\,\delta\tilde{\rho}(r')} \quad (16)$$

For pure density functionals, the arguments of the approximated densities are collapsed. Thus, we obtain[70]

$$f_{\text{xc}}[\tilde{\rho}(r),\tilde{\rho}(r')] \equiv \frac{\delta^2 E_{\text{xc}}[\tilde{\rho}]}{\delta\tilde{\rho}(r)\,\delta\tilde{\rho}(r')}\delta(r - r') = \frac{\delta^2 E_{\text{xc}}[\tilde{\rho}]}{\delta\tilde{\rho}(r)^2} = \frac{\delta^2 v_{\text{xc}}[\tilde{\rho}]}{\delta\tilde{\rho}(r)} \quad (17)$$

The numerical calculation of the kernel matrix elements in ADFT is described in the appendix. With the explicit form for the perturbed exchange-correlation fitting coefficients, we can rewrite the perturbed Kohn−Sham matrix as

$$K_{\mu\nu}^{(\lambda)} = H_{\mu\nu}^{(\lambda)} + \sum_{\bar{k}} \langle\mu\nu||\bar{k}\rangle x_{\bar{k}}^{(\lambda)} + \sum_{\bar{k},\bar{l}} \langle\mu\nu||\bar{k}\rangle F_{\bar{k}\bar{l}}x_{\bar{l}}^{(\lambda)} \quad (18)$$

where

$$F_{\bar{k}\bar{l}} = \sum_{\bar{m}} \langle\bar{k}||\bar{m}\rangle^{-1}\langle\bar{m}|f_{\text{xc}}[\tilde{\rho}]|\bar{l}\rangle \quad (19)$$

Inserting eq 18 via eq 12 into eq 11 yields an explicit expression for the perturbed density matrix in terms of the perturbed fitting coefficients. On the other hand, the derivation of the fitting of eq 4 itself, assuming perturbation-independent basis set and auxiliary functions, yields

$$\sum_{\mu,\nu} P_{\mu\nu}^{(\lambda)}\langle\mu\nu||\bar{m}\rangle = \sum_{\bar{k}} x_{\bar{k}}^{(\lambda)}\langle\bar{k}||\bar{m}\rangle \quad (20)$$

By combining eqs 11, 12, 18, and 20, we then find

$$\sum_{\mu,\nu} P_{\mu\nu}^{(\lambda)}\langle\mu\nu||\bar{m}\rangle = 4\sum_{i}^{\text{acc}}\sum_{a}^{\text{uno}} \frac{\langle\bar{m}||ia\rangle H_{ia}^{(\lambda)}}{\varepsilon_i - \varepsilon_a} + 4\sum_{i}^{\text{acc}}\sum_{a}^{\text{uno}}\sum_{\bar{k}} \frac{\langle\bar{m}||ia\rangle\langle ia||\bar{k}\rangle}{\varepsilon_i - \varepsilon_a}x_{\bar{k}}^{(\lambda)} + 4\sum_{i}^{\text{occ}}\sum_{a}^{\text{uno}}\sum_{\bar{k},\bar{l}} \frac{\langle\bar{m}||ia\rangle\langle ia||\bar{k}\rangle}{\varepsilon_i - \varepsilon_a}F_{\bar{k}\bar{l}}x_{\bar{l}}^{(\lambda)}$$

$$= \sum_{\bar{k}} \langle\bar{m}||\bar{k}\rangle x_{\bar{k}}^{(\lambda)} \quad (21)$$

Thus, the perturbed density can be eliminated and the response equation can be formulated solely in terms of the perturbed fitting coefficients. As a result, the dimension of the corresponding equation system is dramatically reduced, namely, to the number of auxiliary functions, and a direct, noniterative, solution becomes feasible. In order to simplify further notation, we now introduce the perturbation-independent Coulomb and exchange-correlation coupling matrices **A** and **B**. Their elements are given by

$$A_{\bar{k}\bar{l}} \equiv \sum_{i}^{\text{occ}} \sum_{a}^{\text{uno}} \frac{\langle \bar{k}||ia\rangle\langle ia||\bar{l}\rangle}{\varepsilon_i - \varepsilon_a} \tag{22}$$

$$B_{\bar{k}\bar{l}} = \sum_{i}^{\text{occ}} \sum_{a}^{\text{uno}} \sum_{\bar{m},\bar{n}} \frac{\langle \bar{k}||ia\rangle\langle ia||\bar{m}\rangle}{\varepsilon_i - \varepsilon_a} \langle \bar{m}||\bar{n}\rangle^{-1} \langle \bar{n}|f_{\text{xc}}[\tilde{\rho}]|\bar{l}\rangle = \sum_{\bar{m}} A_{\bar{k}\bar{m}} F_{\bar{m}\bar{l}} \tag{23}$$

Similarly, we define the elements of the perturbation vector as

$$b_{\bar{k}}^{(\lambda)} = \sum_{i}^{\text{occ}} \sum_{a}^{\text{uno}} \frac{\langle \bar{k}||ia\rangle H_{ia}^{(\lambda)}}{\varepsilon_i - \varepsilon_a} \tag{24}$$

Inserting these quantities into eq 21 yields

$$(\mathbf{G} - 4\mathbf{A} - 4\mathbf{B})x^{(\lambda)} = 4b^{(\lambda)} \tag{25}$$

Note that the term in parentheses is perturbation-independent and, thus, needs to be calculated only one time. We then find for the perturbed fitting coefficients[39]

$$x^{(\lambda)} = 4(\mathbf{G} - 4\mathbf{A} - 4\mathbf{B})^{-1} b^{(\lambda)} \tag{26}$$

In the case of polarizability calculations, three different perturbation vectors need to be calculated, one for each field component. Once a perturbed fitting coefficient vector is obtained, it is inserted into eq 18 in order to obtain the corresponding perturbed Kohn−Sham matrix. With the perturbed Kohn−Sham matrix, the perturbed density matrix is calculated via the SCP equation (11). Therefore, the final ADPT result is identical with the corresponding CPKS solution. The difference is the elimination of the perturbed density matrix from the response equation system in ADPT. As was already discussed, this is accompanied by a significant reduction of the dimensionality of this equation system and, thus, permits direct, noniterative solutions. From the perturbed density matrix, the polarizability tensor elements are calculated as

$$\alpha_{\lambda\eta} = \sum_{\mu,\nu} P_{\mu\nu}^{(\lambda)} \langle \mu | r_\eta | \nu \rangle \tag{27}$$

where λ denotes the Cartesian component of the electric field and η that of the dipole moment integral.

2.2. NIA-CPKS Method. This approach is a combination of numerical and analytical procedures to solve the CPKS equation. Here the complicated iterative scheme to solve CPKS is avoided. This makes the method practical for use with large molecules and large basis sets. The CPKS equation is the derivative of the Kohn−Sham equation with respect to the electric field.

$$\mathbf{K}^{(\lambda)}\mathbf{c} + \mathbf{K}\mathbf{c}^{(\lambda)} = \mathbf{S}^{(\lambda)}\mathbf{c}\boldsymbol{\varepsilon} + \mathbf{S}\mathbf{c}^{(\lambda)}\boldsymbol{\varepsilon} + \mathbf{S}\mathbf{c}\boldsymbol{\varepsilon}^{(\lambda)} \tag{28}$$

For obtaining a response of electric field, the CPKS equation needs to be solved iteratively, which is a very tedious job. $\mathbf{K}^{(\lambda)}$ constitutes the explicit derivative of the two electron potential terms and the dipole moment operator matrix; this is the bottleneck in obtaining an analytical solution to CPKS. NIA-CPKS gives a single-step solution to CPKS and thus avoids an iterative procedure. For details of implementation, we refer to our previous publication.[33−37] This approach can be used for the closed-shell case only. The elements of the derivative Kohn−Sham matrix are computed as the difference between the elements of the Kohn−Sham matrices calculated at suitably chosen electric field values of around zero.

$$K_{\mu\nu}^{(\lambda)} = \frac{K_{\mu\nu}(+\Delta F_\lambda) - K_{\mu\nu}(-\Delta F_\lambda)}{2\Delta F} \tag{29}$$

Here $K_{\mu\nu}^{(\lambda)}$ is an element of the perturbed Kohn−Sham matrix in the atomic orbital basis. The values $+\Delta F_\lambda$ and $-\Delta F_\lambda$ in parentheses denote the symmetrically chosen field value, and ΔF is the magnitude of the electric field. Using this perturbed Kohn−Sham matrix, the derivative of molecular orbital coefficients $c^{(\lambda)}$ in terms of the atomic orbital basis is obtained analytically by solving the CPKS equation in a single step. The coefficient derivative leads to the first-order perturbed density matrix with the elements

$$P_{\mu\nu}^{(\lambda)} = 2\sum_{i}^{\text{occ}} c_{\mu i}^{(\lambda)} c_{\nu i} + c_{\mu i} c_{\nu i}^{(\lambda)} \tag{30}$$

The NIA-CPKS method for calculating the polarizability has been implemented in revision 1.7 of deMon2k.

TABLE 1: Static Polarizabilities (au) of Azoarene and Disubstituted Azoarene Molecules Calculated with the PBE Functional and GEN-A2* Auxiliary Function Set Using the ADPT, NIA-CPKS, and FFP Methods

	AUXIS			BASIS		
X, Y	ADPT	NIA-CPKS	FFP	NIA-CPKS	FFP	value from ref58
H, H	192.42	192.53	192.91	193.18	193.22	183.82
OH, CN	242.53	242.26	242.84	242.59	242.53	227.98
OH, CHO	243.39	243.28	243.90	243.92	244.05	228.07
OH, NO_2	249.41	249.74	249.91	248.49	249.25	230.35
NH_2, CN	261.73	261.70	262.22	261.82	261.84	247.79
NH_2, CHO	263.70	263.50	264.40	264.42	264.20	246.26
OCH_3, CHO	265.27	265.27	265.84	266.22	266.14	247.03
OCH_3, CN	266.75	266.95	267.26	267.06	267.03	246.88
NH_2, NO_2	271.89	272.23	272.52	271.34	271.70	256.50
OCH_3, NO_2	272.39	272.56	272.95	272.66	272.29	249.86

3. Computational Details

For our comparative study of the azoarene polarizabilities, free azoarene and nine of it para-disubstituted derivatives are studied. The six different substituents, NH_2, OH, CHO, CN, OCH_3, and NO_2, include electron-donating as well as -withdrawing groups. An electron-donating group on one side and an electron-withdrawing group on the other side make azoarene a push−pull system. In order to facilitate a comparison with the calculations of Hinchliffe et al.,[62] the molecular structures were optimized at the B3LYP/6-311++G(2d,1p) level of theory with *GAMESS*. The polarizability values reported in Table 1 were calculated using both NIA-CPKS and ADPT, employing the PBE functional[71] and GEN-A2* auxiliary function sets.[72] In order to study the functional dependency of NIA-CPKS and ADPT polarizabilities, we also employed the local VWN[73] and gradient-corrected BLYP[74,75] functionals. The AUXIS and

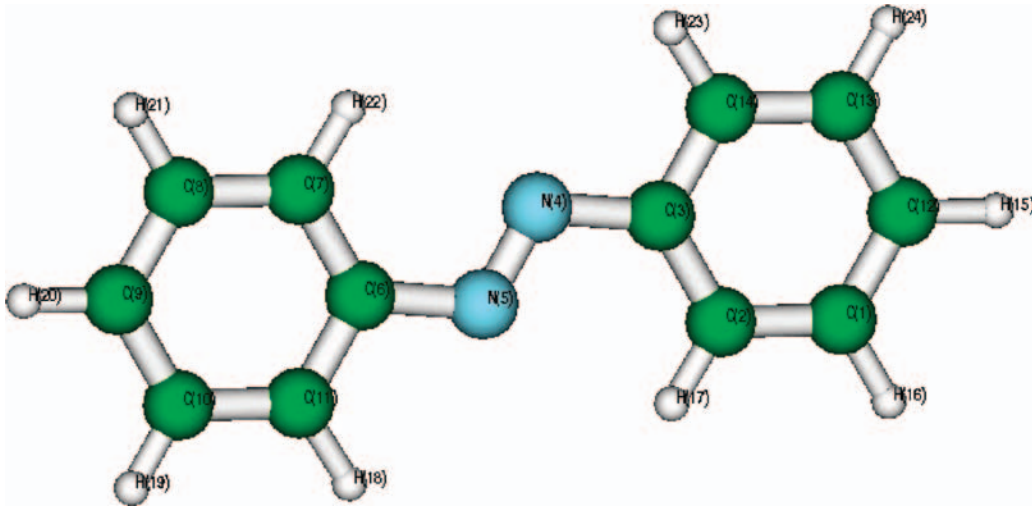

Figure 1. B3LYP/6-311G(2d,1p)-optimized geometry of the parent azoarene molecule.

BASIS options specified in the tables refer to the type of density used for the calculation of the exchange-correlation energy and potential. They are calculated from either the auxiliary functions (AUXIS) or the basis functions (BASIS). Thus, the AUXIS option refers to ADFT and ADPT calculations. Independent of the density used, the exchange-correlation energies and potentials are numerically integrated on an adaptive grid[76] with an accuracy of 10^{-6} au per matrix element. Analytical ADPT polarizabilites are calculated only with the AUXIS option, whereas NIA-CPKS polarizabilities are calculated for both options. In both cases, the Coulomb energy is calculated by the variational fitting procedure proposed by Dunlap et al.[65] For the density fitting, GEN-A2 and GEN-A2* auxiliary function sets are employed. Spherical orbitals are used instead of Cartesian orbitals because they possess no linear dependencies. We used the 6-311++G(2d,2p) basis set throughout the calculations of polarizabilities.

For polarizability calculations employing finite difference methods, the SCF convergence criterion was tightened to 10^{-10} au in all cases. In order to allow a direct comparison, the same convergence criterion was used in the ADPT calculations reported in Table 1. The ADPT polarizabilities in Table 3 were obtained with the default SCF convergence criterion of deMon2k (10^{-6} au). For the FFP calculations, the procedure of Kurtz et al.,[38] as implemented in deMon2k, was applied.[77] As the field strength, the deMon2k default value of 0.032 au was used. For the calculation of the perturbed Kohn−Sham matrix in the NIA-CPKS framework, a field strength of 0.001 au was employed. The average polarizabilities are calculated as normalized traces of the corresponding tensor:

$$\bar{\alpha} = \frac{1}{3}(\alpha_{xx} + \alpha_{yy} + \alpha_{zz}) \tag{31}$$

4. Results and Discussion

In Figure 1, the structure of the parent azoarene molecule is depicted. In the disubstituted derivatives, the substituents X and Y (NH_2, OH, CHO, CN, OCH_3, and NO_2) replace the hydrogen atoms at the 15th and 20th positions. All disubstituted molecules have trans geometry about the azo linkage, and they are nearly planar.[78–80] At this point, it is worth mentioning that azoarenes crystallize in noncentrosymmetric space groups, which ensures the nonlinear activity of the crystals.[81] The polarizabilities calculated using the ADPT, NIA-CPKS, and FFP methods with PBE and GEN-A2* are presented in Table 1 for the sake of comparison. As this table shows, all employed perturbation approaches within deMon2k yield essentially the same results at this level of theory. In particular, the variation between AUXIS and BASIS results, i.e., perturbation calculations with the approximated and exact Kohn−Sham densities, are in the same range as those between analytical and finite-field approaches. This demonstrates the reliability of the analytical, noniterative, ADPT approach. The qualitative order of the azoarene polarizabilities is in all approaches the same.

In Table 1, we also compare our results with the B3LYP values reported by Hinchliffe et al.[60] In general, the B3LYP polarizabilities are smaller than ours. We attribute this mainly to the different functionals used and the basis set that is optimized for the Hartree−Fock-based methods. We emphasize that we used this basis set to facilitate a comparison with other computational approaches. In fact, DFT-optimized basis sets augmented with field-induced polarization functions are much better suited for calculation of the GGA polarizabilities. However, this is not the topic of this report, and we refer the interested reader to the corresponding literature.[10,82,83] By and large, the qualitative trends of the PBE and B3LYP polarizabilities are similar. In detail, we have observed that the smallest enhancement of the polarizability from the parent azoarene molecule is due to the pair OH/CN, which is consistent with the observation of Hinchliffe et al.[60] The largest enhancements are observed for OCH_3/NO_2 and NH_2/NO_2 substitutions. However, among these two pairs, Hinchliffe et al.[60] observed the largest enhancement in NH_2/NO_2, whereas in our calculations, we found that OCH_3/NO_2 shows the largest increment. However, the difference between the increments due to OCH_3/NO_2 and to NH_2/NO_2 is not very large, as observed from Table 1. For other substituents, only minor discrepancies are observed. Unfortunately, experimental values are not available for the systems discussed here.

In Table 2, NIA-CPKS polarizabilities of the studied azoarenes are listed. These calculations were performed with the VWN, BLYP, and PBE functionals in combination with the GEN-A2 and GEN-A2* auxiliary function sets. As this table shows, the NIA-CPKS polarizabilities vary little with respect to the different functionals and auxiliary function sets. The polarizabilities are slightly enlarged if the larger GEN-A2* auxiliary function set is used. With respect to the functional, we note that the VWN

TABLE 2: NIA-CPKS Polarizabilities (au) of Azoarene and Disubstituted Azoarene Molecules Calculated with the VWN, BLYP, and PBE Functionals Using GEN-A2 and GEN-A2* Auxiliary Function Sets

	GEN-A2			GEN-A2*		
X, Y	VWN	BLYP	PBE	VWN	BLYP	PBE
H, H	192.68	193.42	192.04	193.8	194.52	193.18
OH, CN	242.81	242.81	241.81	243.53	243.56	242.59
OH, CHO	244.08	243.76	242.87	245.15	244.92	243.92
OH, NO_2	249.87	249.90	248.28	250.15	250.16	248.49
NH_2, CN	262.57	262.24	261.15	263.04	262.87	261.82
NH_2, CHO	265.28	264.41	263.29	266.11	265.50	264.42
OCH_3, CHO	266.50	265.36	264.61	267.90	266.91	266.22
OCH_3, CN	267.54	266.87	265.93	268.59	267.86	267.06
NH_2, NO_2	272.90	272.44	270.85	273.30	273.56	271.34
OCH_3, NO_2	273.35	272.66	271.03	273.65	273.30	272.66

TABLE 3: ADPT Polarizabilities (au) of Azoarene and Disubstituted Azoarene Molecules Calculated with the VWN, BLYP, and PBE Functionls Using GEN-A2 and GEN-A2* Auxiliary Function Sets

	GEN-A2			GEN-A2*		
X, Y	VWN	BLYP	PBE	VWN	BLYP	PBE
H, H	195.51	194.36	192.14	193.50	194.28	192.40
OH, CN	245.37	244.36	242.21	243.55	244.14	242.36
OH, CHO	247.27	247.27	243.70	244.88	244.27	243.39
OH, NO_2	252.50	254.14	248.96	250.92	251.85	249.41
NH_2, CN	265.96	266.58	262.41	263.31	263.45	261.73
NH_2, CHO	269.17	266.69	264.96	265.54	266.16	263.71
OCH_3, CHO	270.06	267.85	265.51	267.26	267.25	265.28
OCH_3, CN	270.41	268.20	266.42	268.36	268.15	266.75
NH_2, NO_2	277.07	275.88	272.42	273.76	274.19	271.89
OCH_3, NO_2	276.49	273.57	271.70	274.34	274.88	272.38

and BLYP polarizabilities are usually very similar despite the different approximations they represent. On the other hand, the PBE polarizabilities are usually a little bit smaller. The qualitative ordering of the azoarene polarizabilities in Table 2 is for all methods the same. The only exception is the inversion of the NH_2/NO_2- and OCH_3/NO_2-substituted azoarene polarizabilities at the BLYP/GEN-A2* level of theory.

In Table 3, ADPT polarizabilities of the studied azoarenes are listed. The employed methodologies are the same as those in Table 2. By and large, trends similar to those for the NIA-CPKS polarizabilities are observed. Again, the only exceptions in the ordering of Table 1 are inversions in the order of the NH_2/NO_2- and OCH_3/NO_2-disubstituted azoarenes. These inversions are observed for all functionals with the GEN-A2 auxiliary function set in the ADPT calculations. Compared to the NIA-CPKS results, the differences between the ADPT polarizabilities calculated with the GEN-A2 and GEN-A2* auxiliary function sets are larger. This is due to the fact that in ADPT calculations the approximated density is also used for the calculation of the exchange-correlation potential. Obviously, higher-angular-momentum auxiliary functions are needed for the description of the response to the external field. This is also underlined by the ADPT/GEN-A2* polarizabilities, which are for all employed functionals in excellent agreement with their NIA-CPKS/GEN-A2* counterparts. At this point, it is also worth mentioning that the ADPT polarizabilities in Table 3 are obtained with the standard SCF threshold of deMon2k; i.e., no tightening of the SCF procedure was employed. The comparison of the ADPT/PBE/GEN-A2* polarizabilities from Tables 1 and 3 reveals that the SCF tightening is insignificant for the analytical ADPT polarizabilities. Of course, this is in sharp contrast to the numerical methods.

5. Conclusions

In this paper, we present polarizabilities of free and disubstituted azoarenes calculated with the noniterative ADPT and NIA-CPKS methods. In this context, ADPT GGA polarizabilities are reported for the first time. The results obtained are compared to those of standard FFP polarizabilities. We have shown that all three methods give consistent results within a chosen methodology, i.e., a given functional and given basis and auxiliary function sets. In particular, the qualitative ordering of the polarizabilities of the studied azoarenes is very similar with all methodologies. The observed increments in polarizabilities by substitution of the 15th and 20th hydrogen atoms of free azoarene with activating and deactivating groups are in accordance with the standard organic chemistry "activating/deactivating" sequence. Thus, push−pull mechanisms are correctly reproduced at all studied levels of theory. These results underline the reliability of the ADPT approach, in which the perturbation calculation is performed only with the auxiliary density. The direct comparison of the ADPT and NIA-CPKS polarizabilities shows that the difference between the perturbation calculations with the approximated and exact Kohn−Sham density is in the same range as the difference between analytical and finite-field results. Therefore, the errors associated with the ADPT approach are within the intrinsic accuracy of the Kohn−Sham perturbation theory.

Already for medium-sized molecules, like the azoarenes studied here, the differences in the ADPT polarizabilities obtained with the GEN-A2 and GEN-A2* auxiliary function sets are rather small. This fuels the hope that reliable polarizability trends for systems in the nanometer regime are predictable with the ADPT/GEN-A2 level of theory. Our studies also show that NIA-CPKS may be an interesting alternative to the ADPT approach for calculation of the static polarizabilities for very large systems. If GEN-A2* auxiliary function sets are used, the ADPT polarizabilities are in quantitative agreement with the corresponding polarizabilities obtained from the exact perturbed Kohn−Sham density. This strongly motivates the extension of the ADPT approach to other perturbation parameters.

The comparison with the results from Hinchliffe et al. indicates that the incorporation of an exact exchange, as in the B3LYP hybrid functional, changes significantly the polarizability values. For the systems studied here, a decrease is observed. We believe that range-separated hybrid functionals would be even more appropriate for the properties being treated here.[29] This represents an interesting avenue to further improve the DFT polarizabilities and, thus, is a strong motivation for us to incorporate an exact exchange in the ADPT and NIA-CPKS formulation without sacrificing the computational advantages of these methods. Work in this direction is underway in our laboratories. Fukui functions are another type of response properties that can be calculated using both NIA-CPKS and ADPT. There are already ADPT calculations of this response property,[84] and NIA-CPKS can also be further extended.

Appendix

Numerical Kernel Calculation in ADPT. In order to facilitate the implementation and testing of new functionals in the ADPT/ADFT framework, we have implemented the numerical kernel calculation in deMon2k described herein. It allows calculation of exchange-correlation kernels in terms of the corresponding potentials. Thus, only energy and potential expressions need to be implemented for a functional in order to calculate ADPT response properties. In order to derive the

numerical kernel calculation, we start from the definition of the ADPT kernel integrals:

$$\langle \bar{k}|f_{xc}[\tilde{\rho}]|\bar{l}\rangle = \int \bar{k}(r) \int f_{xc}[\tilde{\rho}(r), \tilde{\rho}(r')]\, \bar{l}(r')\, dr'\, dr$$

In order to proceed, we now rewrite the inner integral as

$$\int f_{xc}[\tilde{\rho}(r), \tilde{\rho}(r')]\, \bar{l}(r')\, dr' = \int \frac{\delta v_{xc}[\tilde{\rho}(r)]}{\delta \tilde{\rho}(r')}\, \bar{l}(r')\, dr$$

The right-hand side of the above formula can be expanded as

$$\int \frac{\delta v_{xc}[\tilde{\rho}(r)]}{\delta \tilde{\rho}(r')}\, \bar{l}(r')\, dr' = \lim_{\varepsilon \to 0} \frac{v_{xc}[\tilde{\rho}(r) + \varepsilon \bar{l}(r)] - v_{xc}[\tilde{\rho}(r)]}{\varepsilon}$$

By employing symmetric finite differences, we obtain the following numerical approximation for the inner integral of the exchange-correlation kernel matrix element:

$$\int f_{xc}[\tilde{\rho}(r), \tilde{\rho}(r')]\, \bar{l}(r')\, dr' \cong \frac{v_{xc}[\tilde{\rho}(r) + \varepsilon \bar{l}(r)] - v_{xc}[\tilde{\rho}(r) - \varepsilon \bar{l}(r)]}{2\varepsilon}$$

Substituting this expression back into the original formula for the ADPT kernel matrix elements then yields

$$\langle \bar{k}|f_{xc}[\tilde{\rho}]|\bar{l}\rangle \cong \int \bar{k}(r)\, \frac{v_{xc}[\tilde{\rho}(r) + \varepsilon \bar{l}(r)] - v_{xc}[\tilde{\rho}(r) - \varepsilon \bar{l}(r)]}{2\varepsilon}\, dr$$

Thus, calculation of the ADPT exchange-correlation kernel integrals is reduced to calculation of the corresponding modified exchange-correlation potential integrals. The integral on the right-hand side of the above equation is calculated numerically on the same grid as that used in the SCF calculation. The above finite difference approximation of the kernel integrals is surprisingly robust. From our test calculations, we found that finite difference increments of $\varepsilon = 10^{-9}$ yield excellent results compared to the corresponding CC kernel calculation. Therefore, we have implemented this increment for the numerical kernel calculation in deMon2k.

Acknowledgment. S.P. acknowledges partial financial assistance from SSB and a J. C. Bose fellowship grant toward fulfillment of this work. The authors acknowledge the facilities of the Center of Excellence in Scientific Computing at National Chemical Laboratory. This work was supported by CONACYT (60117), ICYTDF (PIFUTP08-87), and CIAM (107310). J.C.-E. gratefully acknowledges a CONACYT Ph.D. fellowship (208620). This work was performed within the Mexico−Indian Cooperation Project J110.405.

References and Notes

(1) Coleman, A. J. The Force Concept in Chemistry; Deb, B.M., Ed.; Van Nostrand Reinhold: New York, 1981; p 418.
(2) Deb, B. M. *The Force Concept in Chemistry* ; Van Nostrand Reinhold: New York, 1981; p 418.
(3) Dreisler, R. M.; Gross, E. K. U. *Density Functional Theory*; Springer: Berlin, 1990.
(4) Sekino, H.; Bartlett, R. J. *J. Chem. Phys.* **1986**, *84*, 2726.
(5) Sekino, H.; Bartlett, R. J. *J. Chem. Phys.* **1991**, *94*, 3665.
(6) Karna, S. P.; Dupuis, M. *J. Comput. Chem.* **1991**, *12*, 487.
(7) Rice, J. E.; Amos, R. D.; Colwell, S. M.; Handy, N. C.; Sanz, J. *J. Chem. Phys.* **1990**, *93*, 8828.
(8) Kohn, W.; Sham, L. J. *Phys. Rev.* **1965**, *140*, A1133.
(9) Chong, D. P. *J. Chin. Chem. Soc.* **1992**, 39.
(10) Chong, D. P. *Chem. Phys. Lett.* **1994**, *217*, 539.
(11) Duffy, P.; Chong, D. P.; Casida, M. E.; Salahub, D. R. *Phys. Rev. A* **1994**, *50*, 4707.
(12) Guan, J.; Casida, M. E.; Köster, A. M.; Salahub, D. R. *Phys. Rev. B* **1995**, *52*, 2184.
(13) Guan, J.; Duffy, P.; Carter, J. T.; Chong, D. P.; Casida, K. C.; Casida, M. E.; Wrinn, M. *J. Chem. Phys.* **1993**, *98*, 4753.
(14) Jasien, P. G.; Fitzgerald, G. *J. Chem. Phys.* **1990**, *93*, 2554.
(15) Lee, A. M.; Colwell, S. M. *J. Chem. Phys.* **1994**, *101*, 9704.
(16) Sim, F.; Salahub, D. R.; Chin, S. *Int. J. Quantum Chem.* **1992**, *43*, 463.
(17) Dixon, D. A.; Matsuzawa, N. *J. Phys. Chem.* **1994**, *98*, 3967.
(18) Matsuzawa, N.; Dixon, D. A. *J. Phys. Chem.* **1994**, *98*, 2545.
(19) Calaminici, P.; Jug, K.; Köster, A. M.; Ingamells, V. E.; Papadopoulos, M. G. *J. Chem. Phys.* **2000**, *112*, 6301.
(20) Mahan, G. D.; Subbaswamy, K. R. *Local Density Theory of Polarizability*; Plenum Press: New York, 1990.
(21) Gamboa, G. U.; Calaminici, P.; Geudtner, G.; Köster, A. M. *J. Phys. Chem. A* **2008**, *112*, 11969.
(22) Casida, M. E. In *Recent Developments and Applications of Modern Density Functional Theory*; Seminario, M. J., Ed.; Elsevier: Amsterdam, The Netherlands, 1996.
(23) Casida, M. E.; Jamorski, C.; Bohr, F.; Guan, J. *ACS Symp. Ser.* **1996**, *628*, 145.
(24) Casida, M. E.; Wesolowski, T. A. *Int. J. Quantum Chem.* **2004**, *96*, 577.
(25) Görling, A. *Int. J. Quantum Chem.* **1998**, *69*, 265.
(26) Görling, A.; Heinze, H. H.; Ruzankin, S. P.; Staufer, M.; Rösch, N. *J. Chem. Phys.* **1999**, *110*, 2785.
(27) Ipatov, A.; Fouqueau, A.; del Valle, C. P.; Cordova, F.; Casida, M. E.; Köster, A. M.; Vela, A.; Jamorski, C. J. *J. Mol. Struct.: THEOCHEM* **2006**, *762*, 179.
(28) Jamorski, C.; Casida, M. E.; Salahub, D. R. *J. Chem. Phys.* **1996**, *104*, 5134.
(29) Casida, M. E. *J. Mol. Struct.: THEOCHEM* **2009**, *3*, 914.
(30) Casida, M. E. TDDFT for Excited States. In *Computational Methods in Catalysis and Materials Science*; Sautet, P., van Santen, R. A., Eds.; Part of the IDECAT Course Book Series; Wiley-VCH: Weinheim, Germany, 2008; p 33.
(31) Kamiya, M.; Sekino, H.; Tsuneda, T.; Hirao, K. *J. Chem. Phys.* **2005**, *122*, 234111.
(32) Banerjee, A.; Harbola, M. K. *Pramana* **1997**, *49*, 455.
(33) Sophy, K. B. Ph.D. Thesis, University of Pune, Pune, India, 2007.
(34) Sophy, K. B.; Calaminici, P.; Pal, S. *J. Chem.Theory Comput.* **2007**, *3*, 716.
(35) Sophy, K. B.; Pal, S. *J. Chem. Phys.* **2003**, *118*, 10861.
(36) Sophy, K. B.; Pal, S. *THEOCHEM* **2004**, *676*, 89.
(37) Sophy, K. B.; Shedge, S. V.; Pal, S. *J. Phys. Chem. A* **2008**, *112*, 11266.
(38) Kurtz, H. A.; Stewart, J. J. P.; Dieter, K. M. *J. Comput. Chem.* **1990**, *11*, 82.
(39) Flores-Moreno, R.; Köster, A. M. *J. Chem. Phys.* **2008**, *128*, 134105.
(40) Diercksen, G.; McWeeny, R. *J. Chem. Phys.* **1966**, *44*, 3554.
(41) Dodds, J. L.; McWeeny, R.; Raynes, W. T.; Riley, J. P. *Mol. Phys.* **1977**, *33*, 611.
(42) Dodds, J. L.; McWeeny, R.; Sadlej, A. J. *Mol. Phys.* **1977**, *34*, 1779.
(43) McWeeny, R. *Phys. Rev.* **1962**, *126*, 1028.
(44) McWeeny, R. *Methods of Molecular Quantum Mechanics*; Sekino, H., Ed.; Academic Press: London, 2001.
(45) McWeeny, R.; Diercksen, G. *J. Chem. Phys.* **1968**, *49*, 4852.
(46) Flores-Moreno, R. *Analytical Derivatives in LCGTO-DFT Pseudo-Potential Methods with Auxiliary Functions*; Cinvestav: Mexico City, Mexico, 2006.
(47) Köster, A. M.; Calaminici, P.; Casida, M. E.; Flores, R.; Geudtner, G.; Goursot, A.; Heine, T.; Janetzko, F. M.; del Campo, J.; Patchkovskii, S.; Reveles, J. U.; Salahub, D. R.; Vela, A. *deMon2k, The deMon developers*; Cinvestav: Mexico City, Mexico, 2006.
(48) Ågren, H.; Vahtras, O.; Koch, H.; Helgaker, T.; Jørgensen, P. *J. Chem. Phys.* **1993**, *98*, 6417.
(49) Bishop, D. M. *Adv. Chem. Phys.* **1998**, *104*, 1.
(50) Bulat, F. A.; Toro-Labbé, A.; Champagne, B.; Kirtman, B.; Yang, W. *J. Chem. Phys.* **2005**, *123*, 14319.
(51) Champagne, B.; Perpete, E. A.; Jacquemin, D.; van Gisbergen, S. J. A.; Baerends, E. J.; Soubra-Ghaoui, C.; Robins, K. A.; Kirtman, B. *J. Phys. Chem. A* **2000**, *104*, 4755.

(52) Daniel, C.; Dupuis, M. *Chem. Phys. Lett.* **1990**, *171*, 209.
(53) Davis, D.; Sreekumar, K.; Sajeev, Y.; Pal, S. *J. Phys. Chem. B* **2005**, *109*, 14093.
(54) Kanis, D. R.; Ratner, M. A.; Marks, T. J. *Chem. Rev.* **1994**, *94*, 195.
(55) Mikkelsen, K. V.; Luo, Y.; Ågren, H.; Jorgensen, P. *J. Chem. Phys.* **1995**, *102*, 9362.
(56) Morley, J. O. *J. Phys. Chem.* **2002**, *98*, 11818.
(57) Quinet, O.; Champagne, B.; Kirtman, B. *J. Mol. Struct.: THEOCHEM* **2003**, *633*, 199.
(58) Sim, F.; Chin, S.; Dupuis, M.; Rice, J. E. *J. Phys. Chem.* **1993**, *97*, 1158.
(59) Albert, I. D. L.; Morley, J. O.; Pugh, D. *J. Phys. Chem.* **1995**, *99*, 8024.
(60) Hinchliffe, A.; Nikolaidi, B.; Machado, H. J. S. *Int. J. Mol. Sci.* **2004**, *5*, 224.
(61) Jug, K.; Chiodo, S.; Janetzko, F. *Chem. Phys.* **2003**, *287*, 161.
(62) Varanasi, P. R.; Jen, A. K. Y.; Chandrasekhar, J.; Namboothiri, I. N. N.; Rathna, A. *J. Am. Chem. Soc.* **1996**, *118*, 12443.
(63) Boettger, J. C.; Trickey, S. B. *Phys. Rev. B* **1996**, *53*, 3007.
(64) Köster, A. M. *J. Chem. Phys.* **2003**, *118*, 9943.
(65) Dunlap, B. I.; Connolly, J. W. D.; Sabin, J. R. *J. Chem. Phys.* **1979**, *71*, 4993.
(66) Mintmire, J. W.; Sabin, J. R.; Trickey, S. B. *Phys. Rev. B* **1982**, *26*, 1743.
(67) Köster, A. M.; Reveles, J. U.; del Campo, J. M. *J. Chem. Phys.* **2004**, *121*, 3417.
(68) Dunlap, B. I.; Connolly, J. W. D.; Sabin, J. R. *J. Chem. Phys.* **1979**, *71*, 4993.
(69) Köster, A. M.; Calaminici, P.; Gómez, Z.; Reveles, U. J. A Celebration of the Contributions of Robert G. Parr. In *Reviews of Modern Quantum Chemistry*; Sen, K., Ed.; World Scientific: Singapore, 2002.
(70) Gelfand, I. M.; Fomin, S. V. *Calculus of Variations*; Prentice Hall: Englewood Cliffs, NJ, 1963.
(71) Perdew, J. P.; Burke, K.; Ernzerhof, M. *Phys. Rev. Lett.* **1996**, *77*, 3865.
(72) Calaminici, P.; Janetzko, F.; Köster, A. M.; Mejia-Olvera, R.; Zuniga-Gutierrez, B. *J. Chem. Phys.* **2007**, *126*, 044108.
(73) Vosko, S. H.; Wilk, L.; Nusair, M. *Can. J. Phys.* **1980**, *58*, 1200.
(74) Becke, A. D. *Phys. Rev. A* **1988**, *38*, 3098.
(75) Lee, C.; Yang, W.; Parr, R. G. *Phys. Rev. B* **1988**, *37*, 785.
(76) Köster, A. M.; Flores-Moreno, R.; Reveles, J. U. *J. Chem. Phys.* **2004**, *121*, 681.
(77) Calaminici, P.; Jug, K.; Köster, A. M. *J. Chem. Phys.* **1998**, *109*, 7756.
(78) Brown, C. J. *Acta Crystallogr.* **1966**, *21*, 146.
(79) Huang, X.; Kuhn, G. H.; Nesterov, V. N.; Averkiev, B. B.; Penn, B.; Antipin, M. Y.; Timofeeva, T. V. *Acta Crystallogr.* **2002**, *C58*, o624.
(80) Liu, X.-G.; Feng, Y.-Q.; Meng, X.-Q.; Liang, Z.-P.; Yang, G. *Acta Crystallogr.* **2005**, *E61*, o1694.
(81) Adams, H.; Allen, R. W. K.; Chin, J.; O'Sullivan, B.; Styring, P.; Sutton, L. R. *Acta Crystallogr.* **2004**, *E60*, o289.
(82) Calaminici, P. *Chem. Phys. Lett.* **2003**, *374*, 650.
(83) Calaminici, P.; Köster, A. M.; Vela, A.; Jug, K. *J. Chem. Phys.* **2000**, *113*, 2199.
(84) Flores-Moreno, R.; Melin, J.; Ortiz, J. V.; Merino, G. *J. Chem. Phys.* **2008**, *129*, 224105.

JP909966F